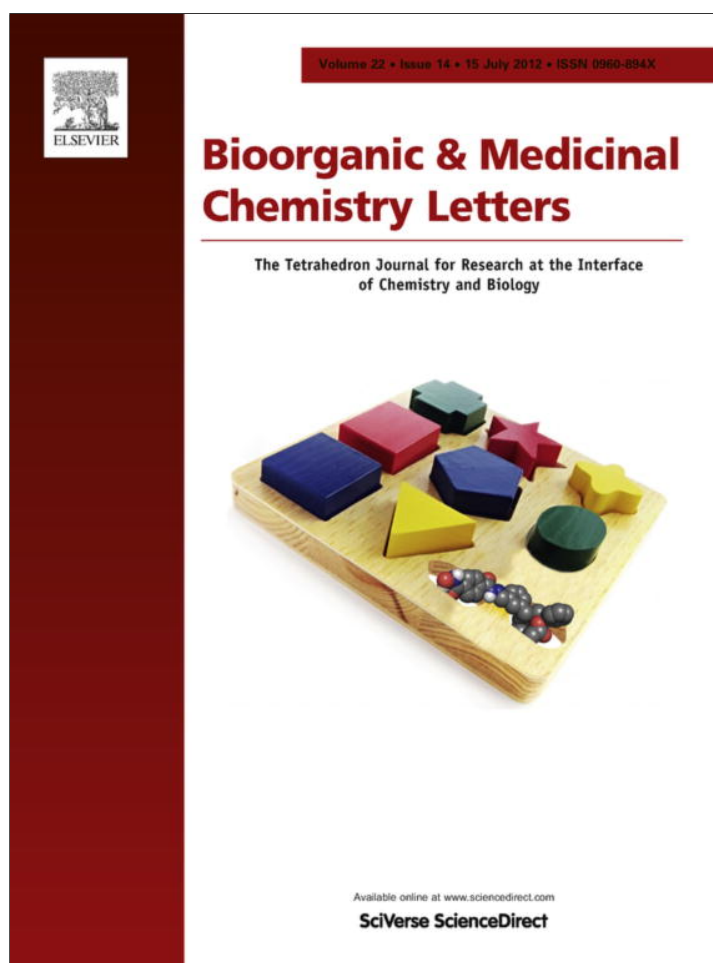


Provided for non-commercial research and education use.
Not for reproduction, distribution or commercial use.



This article appeared in a journal published by Elsevier. The attached copy is furnished to the author for internal non-commercial research and education use, including for instruction at the authors institution and sharing with colleagues.

Other uses, including reproduction and distribution, or selling or licensing copies, or posting to personal, institutional or third party websites are prohibited.

In most cases authors are permitted to post their version of the article (e.g. in Word or Tex form) to their personal website or institutional repository. Authors requiring further information regarding Elsevier's archiving and manuscript policies are encouraged to visit:

<http://www.elsevier.com/copyright>



Contents lists available at SciVerse ScienceDirect

Bioorganic & Medicinal Chemistry Letters

journal homepage: www.elsevier.com/locate/bmcl

CoMSIA and POM analyses of anti-malarial activity of synthetic prodiginines

Devidas T. Mahajan^a, Vijay H. Masand^{a,*}, Komalsing N. Patil^a, Taibi Ben Hadda^b, Rahul D. Jawarkar^c, Sumer D. Thakur^d, Vesna Rastija^e^a Department of Chemistry, Vidya Bharati College, Camp, Amravati, Maharashtra, India^b Laboratoire Chimie des Matériaux, Université Mohammed Premier, Oujda 60000, Morocco^c Department of Pharmaceutical Chemistry, Sahyadri College of Pharmacy, Methwade, Sangola, Solapur, Maharashtra, India^d Department of Chemistry, RDIK College, Badnera, Amravati, India^e Josip Juraj Strossmayer University, Faculty of Agriculture, 31000 Osijek, Croatia

ARTICLE INFO

Article history:

Received 27 January 2012

Revised 23 March 2012

Accepted 11 May 2012

Available online 7 June 2012

Keywords:

CoMSIA

POM analyses

Prodiginines

Anti-malarial activity

ABSTRACT

In present work, 53 synthetic prodiginines were selected to establish thriving CoMSIA (Comparative Molecular Similarity Indices Analysis) model to explore the structural features influencing their anti-malarial activity. POM (Petra/Osiris/Molinspiration) was carried out to get insight into requirements that can lead to the improvement of the activity of these molecules. The CoMSIA model, based on a combination of steric, electrostatic and H-bond acceptor/donor effects, is with $R^2_{cv} = 0.738$ and $R^2 = 0.911$. The analyses reveal that lipophilicity, hydrogen donor/acceptor and steric factors play crucial role. The study with constructive propositions could be useful for the design of new analogues with enhanced activity.

© 2012 Elsevier Ltd. All rights reserved.

Malaria, responsible for more than 2.2 million deaths every year,¹ severely affects the social and economic conditions of patients. Its eradication is still a global challenge due to emergence of resistance against many existing marketed drugs. There is urgent need to either ameliorate the existing drugs or to develop new drugs for this deadly disease. New therapeutics viz. xanthon- es, artemisinins, prodiginines, etc. have been tested against malaria.^{2,5–7}

Prodiginines (Fig. 1), red-pigmented compounds, are linear and cyclic oligopyrrole derivatives that possess wide range of biological activities.^{3,4} Even though potent in vitro activity against Plasmodium species at very low concentration, oral administration, marked parasite clearance and cures in some cases without evident weight loss are some of the advantages associated with prodiginines, search for analogues with better anti-malarial activity, but with reduced toxicity persists.

The mechanism of anti-malarial activity of prodiginines is unknown thereby CoMSIA and other approaches like QSAR, Pharmacophore Modeling, POM, etc. analyses could be complementary tool for drug design. In the present study, we have generated CoMSIA model for a diverse set of prodiginines with an aim to

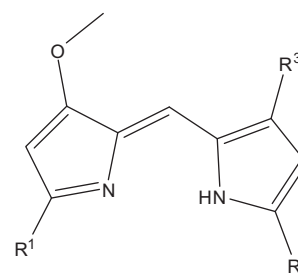


Figure 1. Prodiginines used in present study.

obtain robust model that would provide a hypothetical picture of the chemical features responsible for activity. In addition, POM analysis was also carried out to get better insight into structural requirements. This, in turn, would provide useful understanding for developing potentially new and active drug candidates against *Plasmodium falciparum*.

The 53 prodiginines assayed for in vitro anti-malarial activity against *P. falciparum* pansensitive D6 with chloroquine (CQ) as a reference drug were chosen from literature³ for the present study. These synthetic prodiginines possess diverse substituents like -F, -Cl, alkyl, -NH₂, etc. at different positions. The data reported as IC₅₀ was converted to pIC₅₀ (-log₁₀IC₅₀) to obtain a symmetrically distributed data, which is suitable for smoother PLS regression

Abbreviations: CoMSIA, Comparative Molecular Similarity Indices Analysis; POM, Petra/Osiris/Molinspiration.

* Corresponding author. Tel.: +91 9403312628.

E-mail addresses: vijaymasand@rediffmail.com, vijaymasand@gmail.com (V.H. Masand).

Table 1
Experimental IC₅₀ (nM), pIC₅₀ and predicted pIC₅₀ by CoMSIA

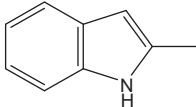
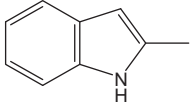
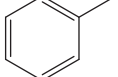
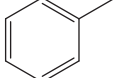
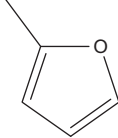
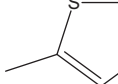
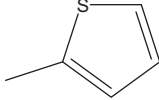
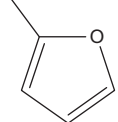
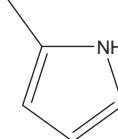
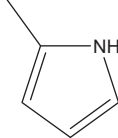
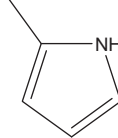
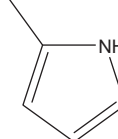
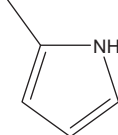
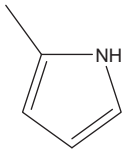
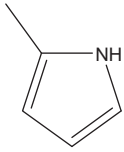
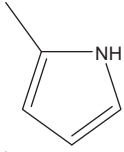
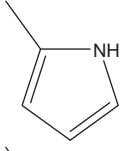
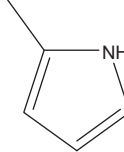
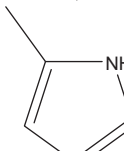
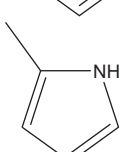
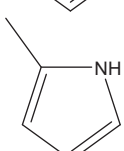
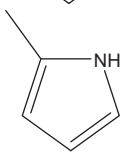
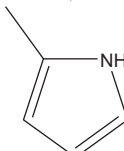
Compd	R ¹	R ²	R ³	IC ₅₀ (nM) D6	pIC ₅₀ expt.	pIC ₅₀ pred. CoMSIA
1		CH ₃	CH ₃	4250	-3.628	-3.696
2		<i>n</i> -C ₁₁ H ₂₃	H	4060	-3.608	-3.472
3		<i>n</i> -C ₁₁ H ₂₃	H	10,470	-4.019	-3.970
4		CH ₃	CH ₃	19,410	-4.288	-3.801
5		<i>n</i> -C ₁₁ H ₂₃	H	2920	-3.465	-3.610
6		CH ₃	CH ₃	>25,000	NC	NC
7		<i>n</i> -C ₁₁ H ₂₃	H	5940	-3.773	-3.749
8		CH ₃	CH ₃	>25,000	NC ^a	NC
9		<i>n</i> -C ₃ H ₇	H	2300	-3.361	-3.260
10		<i>n</i> -C ₄ H ₉	H	1780	-3.250	-3.080
11		<i>n</i> -C ₆ H ₁₃	H	375	-2.574	-2.888
12		<i>n</i> -C ₈ H ₁₇	H	80	-1.903	-2.637
13		<i>n</i> -C ₁₆ H ₃₃	H	300	-2.477	-2.774

Table 1 (continued)

Compd	R ¹	R ²	R ³	IC ₅₀ (nM) D6	pIC ₅₀ expt.	pIC ₅₀ pred. CoMSIA
14		<i>n</i> -C ₁₁ H ₂₂ NH ₂	H	1700	−3.230	−3.219
15		H	(CH ₂) ₃ COOCH ₃	4500	−3.653	−3.625
16		H	CH ₂ CH(CH ₃) ₂	460	−2.662	−2.163
17		H	<i>n</i> -C ₄ H ₉	80	−1.903	−2.134
18		H	<i>n</i> -C ₆ H ₁₃	28	−1.447	−1.462
19		H	<i>n</i> -C ₈ H ₁₇	4.6	−0.662	−1.023
20		H	<i>n</i> -C ₁₀ H ₂₁	8.0	−0.903	−0.811
21		H	<i>n</i> -C ₁₆ H ₃₃	>25,000	NC	NC
22		H	C ₆ H ₅ CH ₂	83	−1.919	−1.913
23		H	4-OCH ₃ C ₆ H ₄ CH ₂	170	−2.230	−2.155
24		H	4-ClC ₆ H ₄ CH ₂	65	−1.812	−1.772

(continued on next page)

Table 1 (continued)

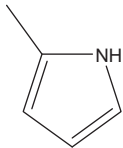
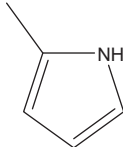
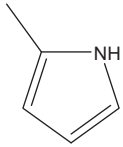
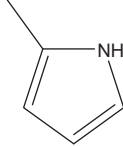
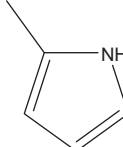
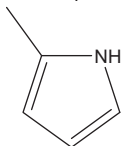
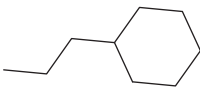
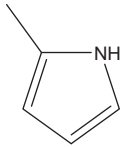
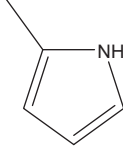
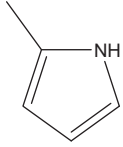
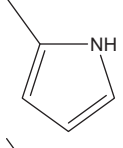
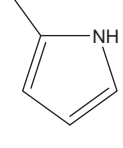
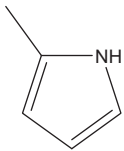
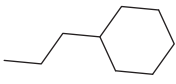
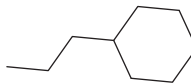
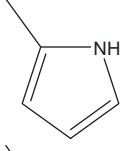
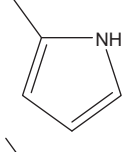
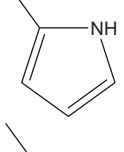
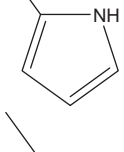
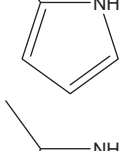
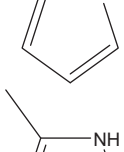
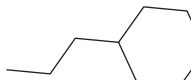
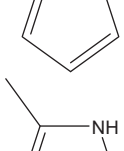
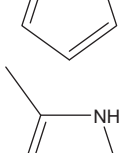
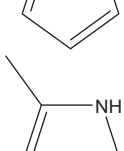
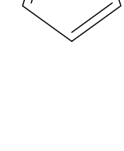
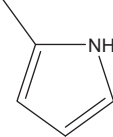
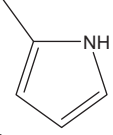
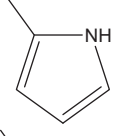
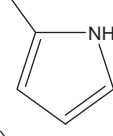
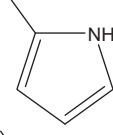
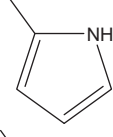
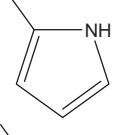
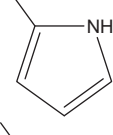
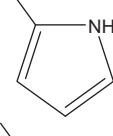
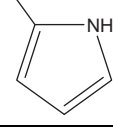
Compd	R ¹	R ²	R ³	IC ₅₀ (nM) D6	pIC ₅₀ expt.	pIC ₅₀ pred. CoMSIA
25		H	4-BrC ₆ H ₄ CH ₂	90	-1.954	-1.598
26		H	2-NaphthylCH ₂	56	-1.748	-1.924
27		CH ₃	CH ₃	8900	-3.949	-3.268
28		<i>n</i> -C ₆ H ₁₃	<i>n</i> -C ₃ H ₇	4.5	-0.653	-1.049
29		<i>n</i> -C ₈ H ₁₇	<i>n</i> -C ₃ H ₇	2.9	-0.462	-1.643
30		<i>n</i> -C ₃ H ₇		1.7	-0.230	-0.073
31		<i>n</i> -C ₆ H ₁₃	<i>n</i> -C ₆ H ₁₃	1.7	-0.230	-0.512
32		<i>n</i> -C ₇ H ₁₅	<i>n</i> -C ₆ H ₁₃	2.1	-0.322	-0.886
33		<i>n</i> -C ₆ H ₁₃	<i>n</i> -C ₈ H ₁₇	4.9	-0.690	-0.328
34		<i>n</i> -C ₇ H ₁₅	<i>n</i> -C ₈ H ₁₇	6.2	-0.792	-0.349
35		<i>n</i> -C ₈ H ₁₇	<i>n</i> -C ₈ H ₁₇	92	-1.963	-1.149

Table 1 (continued)

Compd	R ¹	R ²	R ³	IC ₅₀ (nM) D6	pIC ₅₀ expt.	pIC ₅₀ pred. CoMSIA
36				5.3	-0.724	-0.258
37		C ₂ H ₅	4-ClC ₆ H ₄ CH ₂	6.3	-0.799	-0.799
38		n-C ₃ H ₇	4-ClC ₆ H ₄ CH ₂	3	-0.477	-0.534
39		n-C ₆ H ₁₃	4-ClC ₆ H ₄ CH ₂	2	-0.301	-0.528
40		n-C ₇ H ₁₅	4-ClC ₆ H ₄ CH ₂	2.8	-0.447	-0.555
41		n-C ₈ H ₁₇	4-ClC ₆ H ₄ CH ₂	16	-1.204	-0.566
42		4-ClC ₆ H ₄ CH ₂		3.9	-0.591	-0.357
43		n-C ₆ H ₁₃	4-FC ₆ H ₄ CH ₂	0.9	0.045	-0.622
44		n-C ₈ H ₁₇	4-FC ₆ H ₄ CH ₂	1.3	-0.113	-0.487
45		n-C ₆ H ₁₃	4-BrC ₆ H ₄ CH ₂	2.9	-0.462	-0.504
46		n-C ₈ H ₁₇	4-BrC ₆ H ₄ CH ₂	4	-0.602	-0.386

(continued on next page)

Table 1 (continued)

Compd	R ¹	R ²	R ³	IC ₅₀ (nM) D6	pIC ₅₀ expt.	pIC ₅₀ pred. CoMSIA
47		4-ClC ₆ H ₄ CH ₂	4-ClC ₆ H ₄ CH ₂	6.1	-0.785	-0.779
48		4-FC ₆ H ₄ CH ₂	4-FC ₆ H ₄ CH ₂	5.6	-0.748	-0.951
49		4-BrC ₆ H ₄ CH ₂	4-BrC ₆ H ₄ CH ₂	14	-1.146	-0.659
50		4-FC ₆ H ₄ CH ₂	4-ClC ₆ H ₄ CH ₂	6.1	-0.785	-0.843
51		4-BrC ₆ H ₄ CH ₂	4-ClC ₆ H ₄ CH ₂	8.3	-0.919	-0.758
52		4-BrC ₆ H ₄ CH ₂	4-FC ₆ H ₄ CH ₂	5.7	-0.755	-0.816
53		2,4-Cl ₂ C ₆ H ₃ CH ₂	2,4-Cl ₂ C ₆ H ₃ CH ₂	12.6	-1.100	-0.837
54		2,4-F ₂ C ₆ H ₃ CH ₂	2,4-F ₂ C ₆ H ₃ CH ₂	14.7	-1.167	-0.839
55		3-FC ₆ H ₄ CH ₂	3-FC ₆ H ₄ CH ₂	5.1	-0.707	-0.909
56		2-ClC ₆ H ₄ CH ₂	2-ClC ₆ H ₄ CH ₂	3.6	-0.556	-1.125

^a NC: Not calculated.

analysis.^{5–7} A complete list of compounds is presented in Table 1 along with experimental IC₅₀ (nM), pIC₅₀ and predicted pIC₅₀ by CoMSIA.

All the structures were built and optimized using ACD/ChemSketch 12 Freeware before CoMSIA and POM analyses. To obtain successful results, appropriate alignment of 3D structures is of extreme significance during CoMSIA analysis. The lowest energy conformer (β -isomer) of most active compound **43** was used as

template structure for aligning the total set of molecules using the standard procedure mentioned in manual of SYBYL.^{5–7} Figure 2 represents the alignment of all 53 molecules.

In present analysis, the standard procedure mentioned in the manual of SYBYL was followed to build a database of 53 molecules, PLS analysis and 3D contour generation with optimum number of components set to 4. Default settings and procedure as mentioned in SYBYL were used throughout the work to get the better results.⁸

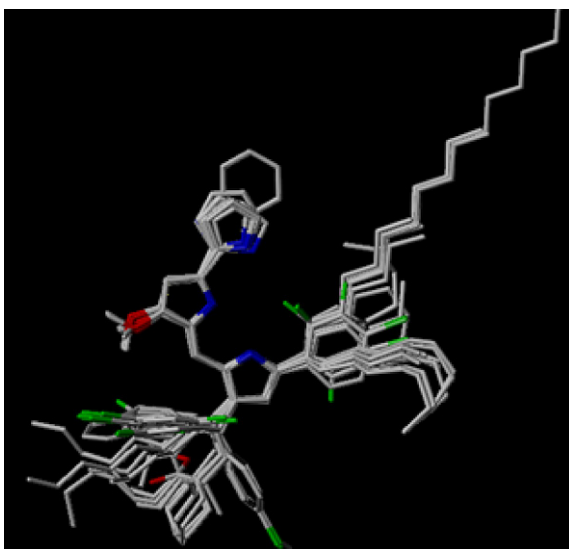


Figure 2. Alignment of compound numbers 1–56 used for CoMSIA.

The CoMSIA model, based on a combination of steric, electrostatic and H-bond acceptor/donor effects, is with $R^2_{cv} = 0.738$, $R^2 = 0.911$, SEE (standard error of estimate) = 0.390, and $F = 122.117$. As shown in Figure 3 (for simplicity, only the structure of compound 43, displaying the highest anti-malarial activity in present series, is depicted as representative), the steric contour map predicts favorable interaction polyhedra (green) around the position R^3 as well as at certain distance from carbon linked with nitrogen of pyrrole ring 3 and unfavorable polyhedra (yellow) in proximity of pyrrole ring 1. This could be one of the reasons for lower activity of compound numbers 1–4. The reliability of steric map calculations is verified by the higher anti-malarial activity of 43 ($IC_{50} = 0.9$ nM) compared to that of 11 ($IC_{50} = 375$ nM) and by the following comparisons: 41 ($IC_{50} = 16$ nM) < 12 ($IC_{50} = 80$ nM), 30 ($IC_{50} = 1.7$ nM) < 9 ($IC_{50} = 2300$ nM), 39 ($IC_{50} = 2.0$ nM) < 40 ($IC_{50} = 2.8$ nM) < 38 ($IC_{50} = 3.0$ nM) < 37 ($IC_{50} = 6.3$ nM) < 41 ($IC_{50} = 16$ nM) < 24 ($IC_{50} = 65$ nM).

The calculated CoMSIA hydrophobic contours (Fig. 4) display favorable hydrophobic substituents (blue polyhedra) near the position R^3 of pyrrole ring 3; hydrophobic substituents become disfavored (red areas) onto heteroatom of ring 1. The reliability of the hydrophobic map calculation is verified by the lower activity of molecule number 6 ($IC_{50} > 25,000$ nM) and 8 ($IC_{50} > 25,000$ nM) compared with 27 ($IC_{50} = 8900$ nM) in which changing the

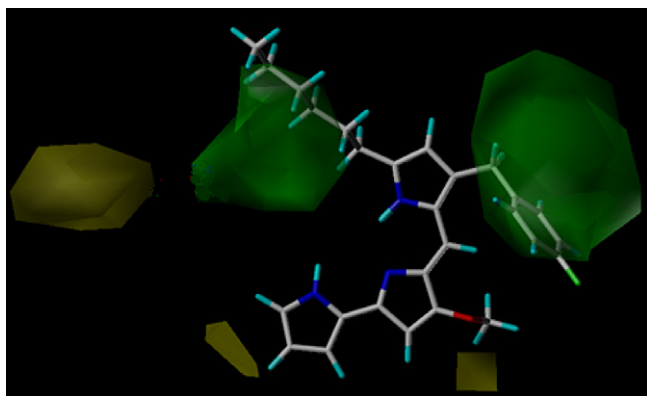


Figure 3. CoMSIA contour maps for steric regions (green: steric favoured, yellow: steric disfavored) displayed around compound 43 (depicted in stick mode and colored by atom type).

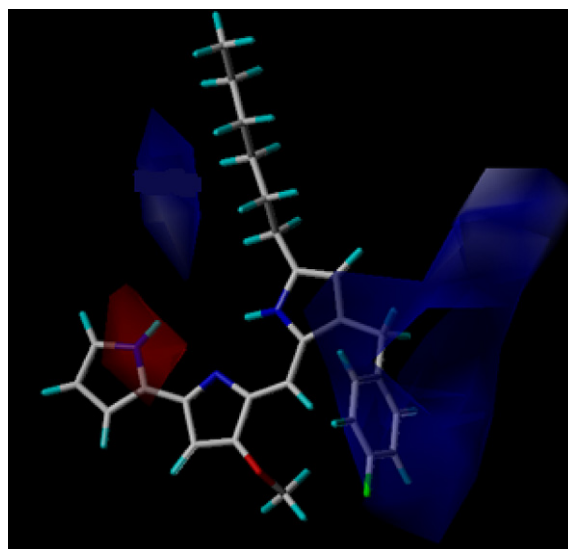


Figure 4. CoMSIA contour maps for hydrophobic regions (blue: hydrophobic favoured, red: hydrophobic disfavored) displayed around compound 43 (depicted in stick mode and colored by atom type).

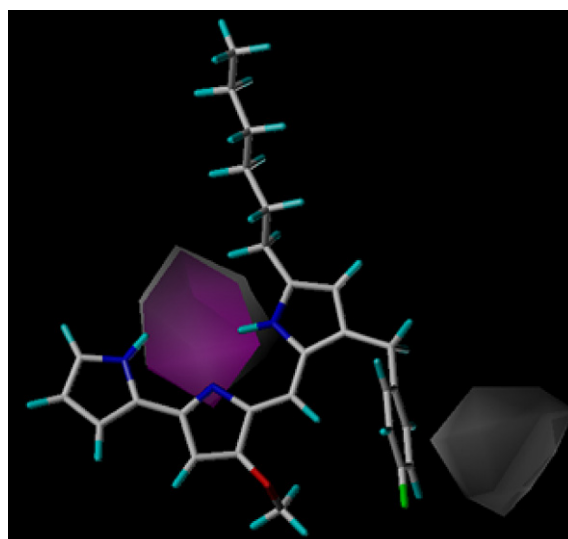


Figure 5. CoMSIA contour maps for hydrogen donor/acceptor regions (cyan: donor favoured, purple: donor disfavored, magenta: acceptor favoured, white: acceptor disfavored) displayed around compound 43 (depicted in stick mode and colored by atom type).

heteroatom from nitrogen to oxygen or sulfur resulted in substantial loss of activity. The reliability of the hydrophobic map calculation is verified by the following trends: 38 ($IC_{50} = 3.0$ nM) < 9 ($IC_{50} = 2300$ nM), 47 ($IC_{50} = 6.1$ nM) < 24 ($IC_{50} = 65$ nM), 49 ($IC_{50} = 14$ nM) < 25 ($IC_{50} = 90$ nM).

Figure 5 illustrates that H-bond acceptor groups are predicted to be beneficial (magenta areas) in proximity of the nitrogen atoms of pyrrole rings. Moreover, H-bond donor functions would be unfavorable (white polyhedra) in proximity of the nitrogen atoms of pyrrole rings and near *ortho* position of aryl nucleus at position R^3 of pyrrole ring 3. Accordingly, compound numbers 5–8 shows lower anti-malarial activity.

A straight line relation between the actual and predicted pIC_{50} indicates that the CoMSIA model has good predictive ability (Fig. 6).

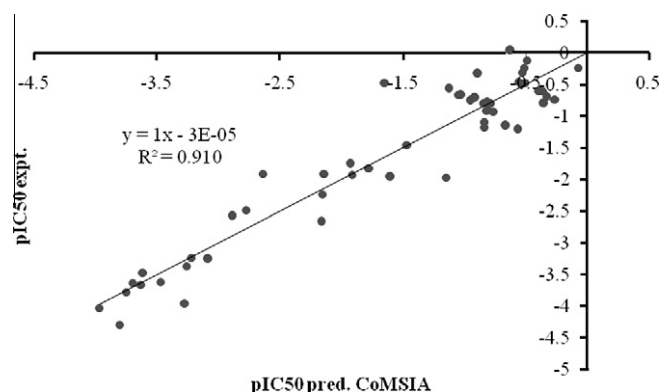


Figure 6. Graph between actual pIC_{50} and predicted pIC_{50} (CoMSIA).

The Osiris Property Explorer, used in present paper is an integral part of ACTELION's inhouse substance registration system. It has the advantage to evaluate impact of lipophilicity on anti-malarial bioactivity of prodiginines (Table 2).

The results of present POM investigation^{9–16} support the suggested structures of prodiginines. It is observed that some substituents such as pyrrole or hetero-aromatics affect the biological activity, which may be due to change in hydrophobic character, liposolubility and metal chelation of the molecules.¹⁷ This, in turn, enhances tridentate coordination character, activity of the

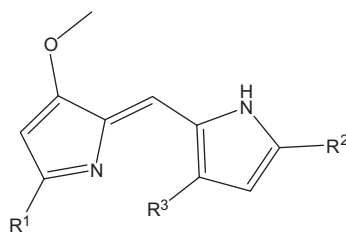
compounds and biological absorbance, so as, most of the natural and synthesized prodiginines have a good antibacterial, antitumor and anti-malarial properties (Table 3).

Several important points emerge from Tables 2 and 3 concerning the coordinative, electronic, lipophilicity and steric factors which have direct impact on bioactivity properties. The positive results we have recorded, concerning the nature of substituent R^3 (pyrrole ring), while encouraging for purposes of new drug design, confirm that very likely most of these compounds could be used as potential tridentate ligand with good anti-malarial activity after minor modifications (Fig. 7). From Figure 7, it is clear that the conversion of β -isomer to other form is possible; this inter-conversion may be useful in adopting appropriate bio-active conformation to enhance anti-malarial activity of prodiginines.

Based on their structural properties, these compounds may be useful as chelating N,N,N-ligands with potential bioactivity.¹⁷ These results prompt several pertinent observations: (i) This type of tri-pyrrole system can furnish an interesting model for studying the interaction of antibiotics with viral target because of the possible charge modification of substituents (R^1 , R^2 , R^3) and N/N/N of pharmacophore group; (ii) The future flexible pharmacophore site(s) geometric conformation will enable us to prepare [Ruthenium (II)-(prodiginine)_n] complexes for multi-therapeutic materials with high selectivity. In fact, their ability to play as N,N,N-tridentate ligands confers them to act as potential stable ligands leading us to obtain in situ the [(L)_n-Metal-OH₂] complexes with controlled redox properties.^{17,18}

Table 2

Osiris calculations⁸ of four most active compounds (30, 31, 43, 44) and four less active compounds (3, 4, 7, 27)



Compd	Substituents			Osiris calculations ^a				
	R^1	R^2	R^3	MW	$cLogP$	S	DL	D-S
3	CH ₃	CH ₃	C ₆ H ₅	404	7.53	-6.56	-16.05	0.14
4	C ₁₁ H ₂₃	H	C ₆ H ₅	278	3.32	-4.31	1.84	0.69
7	C ₁₁ H ₂₃	H	C ₄ H ₃ S	410	7.38	-6.575	-16.7	0.14
27	CH ₃	CH ₃	C ₄ H ₄ N	267	2.09	-3.36	0.53	0.57
30	C ₆ H ₁₃	C ₆ H ₁₃	C ₄ H ₄ N	407	6.52	-5.84	-14.40	0.13
31	C ₃ H ₇	C ₃ H ₇	C ₄ H ₄ N	391	4.96	-5.54	-6.35	0.18
43	C ₆ H ₁₃	<i>p</i> -F-C ₆ H ₄ CH ₂	C ₄ H ₄ N	431	5.78	-6.28	-14.90	0.14
44	C ₈ H ₁₇	<i>p</i> -F-C ₆ H ₄ CH ₂	C ₄ H ₄ N	459	6.71	-6.82	-17.71	0.11

^a S: solubility, DL: drug-likeness, D-S: drug-score, $cLogP$: $LogP$ calculated by Osiris.

Table 3

Molinspiration calculations of four most active compounds (30, 31, 43, 44) and four less active compounds (3, 4, 7, 27)

Compd	Molinspiration calculations ^a				Drug-likeness ^b			
	$cLogP$	TPSA	OH–NH Interact.	Volume	GPCRL	ICM	KI	NRL
3	8.56	38	1	418	0.12	-0.12	0.19	-0.02
4	3.98	75	1	266	-0.14	-0.36	0.37	-0.21
7	8.45	38	1	409	0.03	-0.17	0.18	-0.10
27	2.78	54	2	251	-0.12	-0.12	0.56	-0.12
30	7.85	54	2	419	0.17	-1.15	0.35	-0.03
31	6.57	54	2	392	0.19	-0.15	0.30	0.09
43	7.01	54	2	412	0.21	-0.09	0.39	0.13
44	8.10	54	2	446	0.20	-0.08	0.36	0.09

^a TPSA: total molecular polar surface area. $cLogP$: $LogP$ calculated by Molinspiration.

^b GPCRL: GPCR ligand; ICM: ion channel modulator; KI: kinase inhibitor; NRL: nuclear receptor ligand.

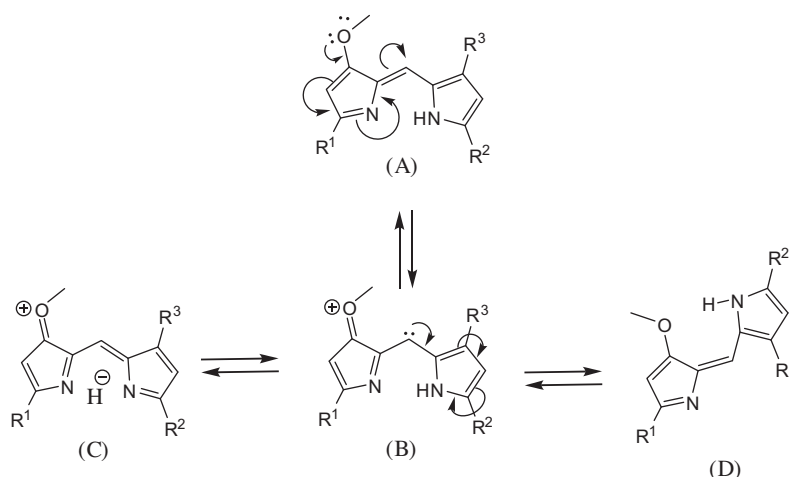


Figure 7. *Z/E* geometric isomerism of prodiginines (A to D).

The 3D-QSAR and POM analyses presented here emphasize the key structural features impacting the anti-malarial activity of prodiginines. Moreover, they insinuate constructive hints for the design of new analogues with improved activity. The models could be used to design new ligands with better activity, before their synthesis.

Acknowledgments

We are thankful to ACD labs development team for providing trial version of their software. We are thankful to NIPER, Chandigarh and CDRI, Lucknow to allow doing the computational work. Professor T. Ben Hadda would like to thank ACTELION; the Biopharmaceutical Company of Swiss, for the online molecular properties calculations and to Ministry of High Science and Education for financial support.

References and notes

- WHO report; 2010.
- Masand, V. H.; Patil, K. N.; Nazerruddin, G. M.; Jawarkar, R. D.; Bajaj, S. O. *Org. Chem. Ind. J.* **2010**, *6*, 30.
- Papireddy, K.; Smilkstein, M.; Kelly, J. X.; Shweta; Salem, S. M.; Alhamadsheh, M.; Haynes, S. W.; Challis, G. L.; Reynolds, K. A. *J. Med. Chem.* **2011**, *54*, 5296.
- Williamson, N. R.; Fineran, P. C.; Leeper, F. J.; Salmond, G. P. C. *Nat. Rev.* **2006**, *4*, 887.
- Masand, V. H.; Jawarkar, R. D.; Mahajan, D. T.; Hadda, T. B.; Sheikh, J.; Patil, K. N. *Med. Chem. Res.*, in press doi: <http://dx.doi.org/10.1007/s00044-011-9787-x>.
- Jawarkar, R. D.; Masand, V. H.; Patil, K. N.; Mahajan, D. T.; Youssoufi, M. H.; Hadda, T. B.; Der Kumbhare, S. L. *Pharm. Chem.* **2010**, *2*, 302.
- Jawarkar, R. D.; Masand, V. H.; Mahajan, D. T.; Hadda, T. B.; Der Kurhade, G. H. *Pharm. Chem.* **2010**, *2*, 350.
- The aligned molecules, **43** as reference molecule, were placed in a 3D cubic lattice with a grid spacing of 2.0 Å in the *x*, *y*, and *z* directions. The steric (Lennard–Jones potential) and electrostatic (Coulombic potential) field energies were calculated at each grid point using a Tripos force field. The energies were truncated to +30 kcal/mol. A probe atom *sp*³ carbon with charge +1, hydrophobicity +1, and H-bond donor and H-bond acceptor property of +1 was placed at every grid point to measure the five CoMSIA fields. A default value of 0.3 was used as an attenuation factor. The cross-validation analysis was performed using the 'leave-one-out' (LOO) method. The optimum number of components obtained from the LOO method was applied to derive the final non-cross-validated correlation *R*².
- Fathi, J.; Masand, V. H.; Jawarkar, R. D.; Mouhoub, R.; Hadda, T. B. *J. Comput. Method Mol. Des.* **2011**, *1*, 57.
- Jarrahpour, A.; Fathi, J.; Mimouni, M.; Hadda, T. B.; Sheikh, J.; Chohan, Z. H.; Parvez, A. *Med. Chem. Res.* **2011**, *19*, 1. <http://dx.doi.org/10.1007/s00044-011-9723-0>.
- Rauf, A.; Ahmed, F.; Qureshi, A. M.; Aziz-ur-Rehman; Khan, A.; Qadir, M. I.; Choudhary, M. I.; Chohan, Z. H.; Youssoufi, M. H.; Hadda, T. B. *J. Chin. Chem. Soc.* **2011**, *58*, 1.
- Sheikh, J.; Parvez, A.; Ingle, V.; Juneja, H.; Dongre, R.; Chohan, Z. H.; Youssoufi, M. H.; Hadda, T. B. *Eur. J. Med. Chem.* **2011**, *46*, 1390.
- Hadda, T. B.; Badri, R.; Kerbal, A.; Baba, B. F.; Akkurt, M.; Demailly, G.; Benazza, M. *ARKIVOC* **2007**, *xvi*, 276.
- Parvez, A.; Jyotsna, M.; Youssoufi, M. H.; Hadda, T. B. *Phosphorus, Sulfur Silicon Relat. Elem.* **2010**, *7*, 1500.
- Jarrahpour, A.; Motamedifar, M.; Zarei1, M.; Youssoufi, M. H.; Mimouni, M.; Chohan, Z. H.; Hadda, T. B. *Phosphorus Sulfur Silicon Relat. Elem.* **2010**, *185*, 491.
- Bennani, B.; Kerbal, A.; Daoudi, M.; Filali, B.; Al Houari, G.; Jalbout, A. F.; Mimouni, M.; Benazza, M.; Demailly, G.; Akkurt, M.; Öztürk, Y. S.; Hadda, T. B. *ARKIVOC* **2007**, *xvi*, 19.
- Gale, P. A.; Dehaen, W. *Anion Recognition in Supramolecular Chemistry (Topics in Heterocyclic Chemistry)*; Springer: New York, 2010.
- Hadda, T. B.; Akkurt, M.; Baba, M. F.; Daoudi, M.; Bennani, B.; Kerbal, A.; Chohan, Z. H. *J. Enzyme Inhib. Med. Chem.* **2008**, *24*, 457.